Dalton Transactions

Dynamic Article Links

Cite this: *Dalton Trans.*, 2011, **40**, 9868

www.rsc.org/dalton

PAPER

Coordination of uranium(VI) with functional groups of bacterial lipopolysaccharide studied by EXAFS and FT-IR spectroscopy†

Astrid Barkleit,* Harald Foerstendorf, Bo Li, André Rossberg, Henry Moll and Gert Bernhard

Received 31st March 2011, Accepted 18th July 2011
DOI: 10.1039/c1dt10546a

The complexation of uranyl ions with lipopolysaccharide (LPS), the main component of the cell wall of Gram-negative bacteria, was investigated on a molecular level with U L_{III}-edge extended X-ray absorption fine structure (EXAFS) and attenuated total reflection Fourier transform infrared (ATR-FT-IR) spectroscopy over a wide pH range (2.6 to 7.0). For the first time, structural determinations of uranyl complexes with cell wall compounds were extended from acidic up to neutral pH. The main functionalities responsible for uranyl binding are phosphoryl and carboxyl groups. At an excess of LPS, related to environmental conditions, the uranyl ion is mainly complexed by phosphoryl groups four-fold monodentately coordinated in the equatorial plane of the uranyl dioxo cation UO_2^{2+} showing great homologies to the uranyl mineral phase *meta*-autunite in the EXAFS spectra. At equimolar ratios of uranyl and functional groups of LPS, according to a slight deficit of phosphoryl groups, additional carboxyl coordination in a bidentate manner becomes important as it is shown by IR spectroscopy. From the vibrational spectra, a mixed coordination of UO_2^{2+} with both phosphoryl and carboxyl groups is derived. The coordination of uranyl ions to the LPS molecule is obviously mainly controlled by the U/LPS concentration ratio, and the influence of pH is only of minor significance at the investigated range.

Introduction

Microorganisms have a great potential for environmental bioremediation processes because of their pronounced capability to adsorb and deposit high amounts of (radio-)toxic metal ions. In uranium contaminated areas, not only living bacteria but also lysed dead cells can influence the migration behaviour of uranium by releasing significant quantities of biopolymers, such as cell siderophores, polypeptides, phosphorylated peptides, cell wall components or nucleic acids. These biomolecules are potentially able to bind considerable amounts of uranium. Therefore, a detailed understanding of the binding mechanisms of the metal ions is required for a comprehensive description of the radionuclide transport mechanisms in the environment and for the improvement of technical bioremediation strategies at a molecular level.[1–4]

It can be suggested that the capability of microorganisms to bind high amounts of contaminants dissolved in the aqueous phase is due to the chemical properties of their cell walls because they constitute the outer shell of the organisms. The great number of charged functional groups generally facilitates an efficient complexation of metal ions.[1–4] One of the main components of the cell wall of Gram-negative bacteria is lipopolysaccharide (LPS). It is embedded in the outer membrane and is exposed to the environment of the microbe. LPS plays a key role in specific interactions with metal ions in the environment. The capability of metal complexation is suggested to be based on the high density of functionalities, mainly carboxyl and phosphoryl groups. The LPS molecule can be divided into three main regions: (a) the lipid A, which is integrated in the membrane, (b) the core region, containing the majority of the functional groups, which are supposed to be responsible for high capability of metal binding, and (c) the repeating unit, the O-antigen[5] (Fig. 1).

In our recent study,[6] we investigated the interaction of uranium with LPS of *Pseudomonas aeruginosa* using potentiometric titration and time-resolved laser-induced fluorescence spectroscopy (TRLFS). We identified several uranyl LPS complexes and assumed that the uranyl ion is mainly coordinated to phosphoryl groups. In addition, it was supposed that the coordination of uranyl to carboxyl groups becomes dominant when the number of available phosphoryl groups is deficient. These results are in accordance with earlier findings where the high affinity of uranium to phosphoryl groups[7–14] and the additional coordination to carboxyl groups[15–17] have been demonstrated in several microbial systems as well as animal and human (renal and bone) cell systems[18–20] at low to slightly acidic pH.

In a recent computer simulation study of uranyl uptake by LPS at neutral pH the retention of uranyl ions by formation of chelate complexes with carboxyl and hydroxyl groups was

Helmholtz-Zentrum Dresden-Rossendorf e.V., Institute of Radiochemistry, P.O. Box 510119, 01314 Dresden, Germany. E-mail: a.barkleit@hzdr.de; Fax: +49 351 260 3553; Tel: +49 351 260 3136

† Electronic supplementary information (ESI) available: Description of the EXAFS analysis of minor scattering contributions and luminescence spectroscopy (experimental and spectra). See DOI: 10.1039/c1dt10546a

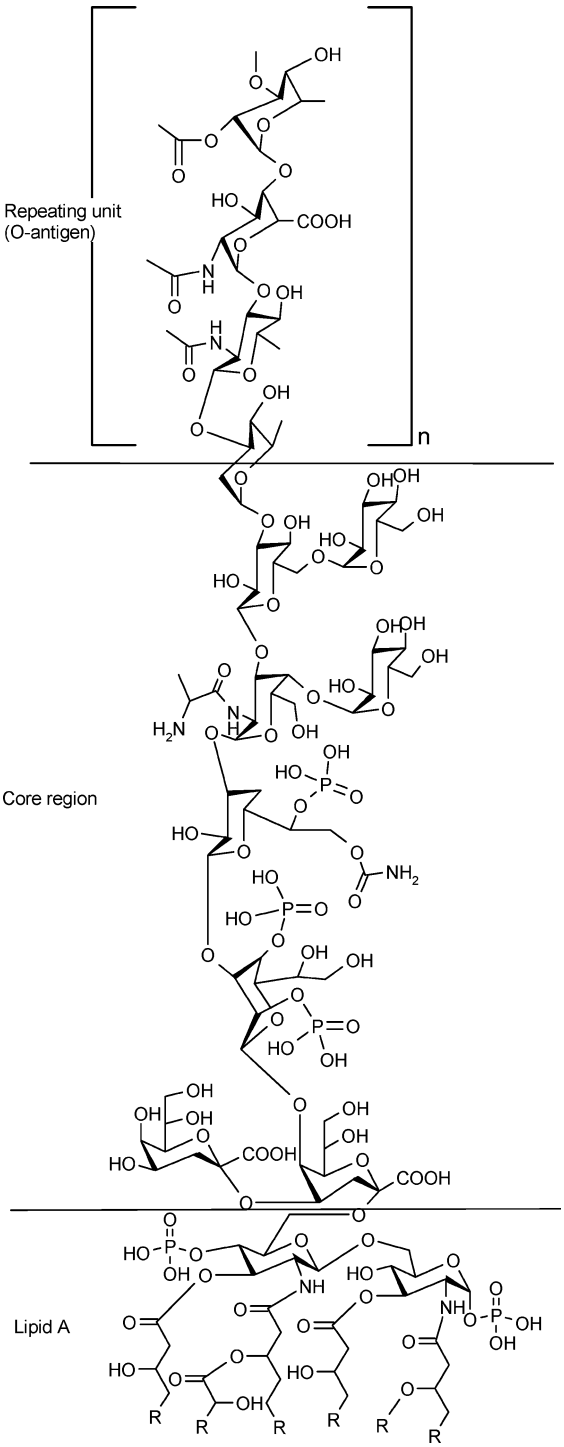

Fig. 1 Chemical structure of LPS from *Pseudomonas aeruginosa* S10.

predicted.[21] A verification of the complexation behaviour of uranyl with LPS at slightly acidic to neutral pH with the aid of further spectroscopic techniques has become necessary. From our previous study,[6] structural information of the postulated uranyl LPS complexes could not be derived. The techniques applied, that is potentiometric titration and TRLFS, only provide quantitative information of the number of complex species, stability constants and distribution of the species. Therefore, in this continuative work, we investigated the uranyl complexes with LPS in order to identify the coordinating functional groups under different pH and stoichiometric conditions. For the discrimination between potential functional groups, namely carboxyl and phosphoryl groups, extended X-ray absorption fine structure (EXAFS) spectroscopy at the U L_{III}-edge and attenuated total reflection Fourier-transform infrared (ATR-FT-IR) spectroscopy were applied. EXAFS is used to probe the interatomic distances of the cation, whereas FT-IR provides molecular information of both the ligand and the uranyl ion. With respect to the applicability of both techniques, samples with an excess of LPS reflecting typical environmental conditions, were investigated by EXAFS. Furthermore, samples with equimolar ratios up to an excess of uranyl to LPS functional groups were prepared. Because EXAFS provides ambiguous results under these experimental conditions, IR measurements were carried out to gain more detailed information about the functional groups involved in U(VI) complexation in these samples.

Experimental section

Materials

For EXAFS experiments, a stock solution of UO_2^{2+} was made from $UO_2(ClO_4)_2 \cdot 6H_2O$ (Merck, p.A.). A UO_2Cl_2 stock solution, prepared as described in ref. 22, was used for IR spectroscopy. LPS from *Pseudomonas aeruginosa* S10 were purchased from Sigma. The molar ratios of the functional groups of LPS (carboxyl and phosphoryl) were calculated from the site densities obtained from potentiometric titration experiments.[6] Adjustments of pH were accomplished by adding aliquots of 1 M NaOH, $HClO_4$ or HCl (FT-IR) with an accuracy of 0.02 units. The ionic strength was kept constant at 0.1 M (NaCl) for the solutions (FT-IR). All solutions were prepared with carbonate-free deionized water.

EXAFS spectroscopy

For sample preparation, 0.75 mL 13.3 mM (sample A, B, and C) or 66.5 mM (sample D) UO_2^{2+} solution were added dropwise to 100 mg solid LPS each (according to about 30 μmol carboxyl and phosphoryl groups each). At first, the pH was adjusted to the required value (see Table 1), then the suspensions were shaken for 3 h, evaporated at room temperature to obtain a suspension with a volume of about 150 μL (for final sample composition, see Table 1), packed in a Teflon® sample holder, shock-frozen and stored in liquid nitrogen. EXAFS experiments of aqueous solutions with U(VI) concentration levels as used for IR spectroscopy failed because of the very low signal-to-noise ratio. Therefore, samples containing higher uranyl concentrations as given in Table 1 were necessary.

EXAFS measurements were carried out at the Rossendorf Beamline at the European Synchrotron Radiation Facility[23] in a closed cycle helium cryostat at 15 K. The U L_{III}-edge fluorescence spectra were measured with a 13-element germanium detector. Eight spectra for each measurement were recorded and then averaged. For energy calibration of the sample spectra, the *K*-edge spectrum of an yttrium foil (17038 eV) was recorded simultaneously. The U L_{III}-edge ionization potential was defined as 17185 eV. The EXAFS spectra were analyzed according to standard procedures including statistical weighting of the 13 fluorescence channels and dead-time correction using EXAFSPAK.[24]

Table 1 Composition of all uranyl LPS EXAFS and FT-IR samples. The molar ratios of the functional groups of LPS (carboxyl and phosphoryl) were calculated from the site densities determined with potentiometric titration[6]

Sample	pH	UO_2^{2+}	LPS	U : P : C ratio
EXAFS (suspension)				
A	2.6	10 µmol	100 mg (30 µmol OPO_3H and COOH each)	1 : 3 : 3
B	4.6	10 µmol	100 mg	1 : 3 : 3
C	7.0	10 µmol	100 mg	1 : 3 : 3
D	3.9	50 µmol	100 mg	5 : 3 : 3
FT-IR (solution)				
E	2.7	1.0 mM	1 g L^{-1} (0.3 mM OPO_3H and COOH each)	3 : 1 : 1
F	4.5	0.1 mM	0.17 g L^{-1} (0.05 mM OPO_3H and COOH each)	2 : 1 : 1
G	7.0	0.2 mM	0.34 g L^{-1} (0.1 mM OPO_3H and COOH each)	2 : 1 : 1

Theoretical phase and amplitude functions were calculated with the software FEFF 8.2[25] by using X-ray data from *meta*-autunite, $Ca(UO_2)_2(PO_4)_2{\cdot}6H_2O$,[26] and sodium tris(acetato)dioxouranate, $Na(UO_2)(CH_3COO)_3$.[27]

ATR-FT-IR spectroscopy

The measurements of pure LPS in aqueous solution (2 g L^{-1}; 0.1 M NaCl) were carried out at pH 3.0, 5.0, 7.0 and 9.0. The uranyl LPS complex solutions were prepared by adding an appropriate amount of $U(VI)_{aq}$ to dissolved LPS, and subsequent adjustment of the pH until the final values were obtained (see Table 1; 0.1 M NaCl each). The final concentrations were restricted due to the solubility of the complexes at the required pH values. All measurements were repeated twice for reproducibility. Experiments of uranyl LPS suspensions with a low U/LPS ratio, comparable to the EXAFS samples, failed because of the outstanding intensities of the vibrational modes of the sugar units of LPS.

The infrared spectra were recorded at room temperature with an FT-IR spectrometer (Bruker VERTEX 80/v) equipped with a diamond ATR cell (crystal diameter: 4 mm, 9 reflections; Smiths Inc.) and an MCT detector. For the complex species, difference spectra were calculated from single-beam spectra consecutively recorded from solutions containing the uranyl LPS complexes and pure LPS with the same concentration and pH. For the experiments, an ATR flow cell (volume: 200 µL) with a constant flow rate of 200 µL min^{-1} was used. Each single-beam spectrum was co-added from 128 scans at a spectral resolution of 4 cm^{-1}.

Results and discussion

EXAFS measurements

Fig. 2 shows the raw U L_{III}-edge k^3-weighted EXAFS spectra of the uranyl LPS samples (A: pH 2.6, B: pH 4.6, C: pH 7.0, all with excess of phosphoryl groups; D: pH 3.9 with deficit of phosphoryl groups) and the corresponding Fourier transform (FT). The best theoretical fits derived from the model compounds are included (see experimental section). For comparison, the spectrum of *meta*-autunite, a uranyl phosphate mineral with a well-known crystal structure,[26] is provided (Fig. 2, trace at top). The EXAFS structural parameters are summarized in Table 2. During the fit procedure, the coordination number (N) of the axial oxygen atoms (O_{ax}) was fixed to two. The two-fold degenerate 4-legged multiple scattering path along the uranyl linear unit, $U–O_{ax(1)}–U–O_{ax(2)}$, was considered in the fit procedure. The $U–O_{ax}$ distances of about 1.79 Å obtained are typical values of uranyl compounds.[28]

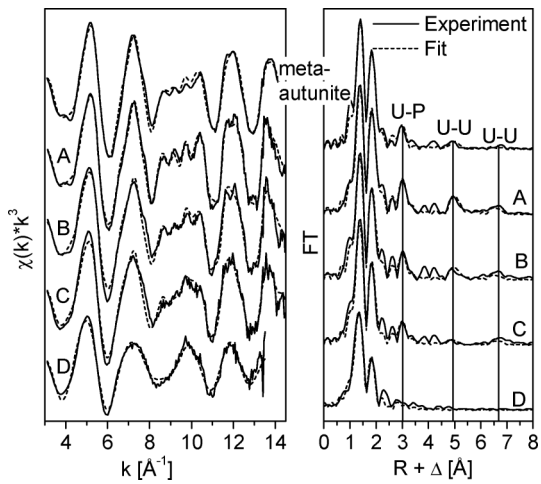

Fig. 2 Left: Raw U L_{III}-edge k^3 weighted EXAFS spectra of uranyl LPS complexes including the best theoretical fits. Sample A: U : P = 1 : 3, pH = 2.6; B: U : P = 1 : 3, pH = 4.6; C: U : P = 1 : 3, pH = 7.0; D: U : P = 5 : 3, pH = 3.9 (compositions see Table 1); and *meta*-autunite. Right: Corresponding Fourier transforms. Labels indicate the assignments to interatomic distances (see Table 2).

The spectra of the samples A and B with an excess of functional groups of LPS (according to a threefold molar excess of phosphoryl to uranyl) are quite similar irrespective of the initial pH. In addition, the spectra are in good agreement with those of *meta*-autunite. The spectrum of sample C with an excess of functional groups of LPS at pH 7.0 shows all spectral features as obtained for the samples A and B, but shows slight differences in the EXAFS pattern between 8.5 and 10.5 $Å^{-1}$. Note that at pH 7.0 nearly all carboxylic groups are deprotonated and might also contribute to interactions with U(VI) (see Fig. 3). Therefore, we cannot exclude that at pH 7.0 a second species coexists in a minor amount which may slightly influence the spectrum. However, the structural parameter observed for sample C are in good accordance with those obtained for the samples A and B and generally match the structural parameter observed for *meta*-autunite.

For samples A, B and C, very short $U–O_{eq}$ distances of 2.28 Å to 2.30 Å with a coordination number of about 4 are obtained in the first equatorial shell. Strong signals at about 3 Å in the FT are due

Table 2 EXAFS fitting parameters

Sample	Shell	CN^a	R/Å^b	σ^2/Å^{2c}	ΔE_0/eV^d	F^e
meta-autunite	U═O	2^f	1.79	0.0017	2.4	0.16
	U–O_{eq}	4^f	2.29	0.0029	2.4^g	
	U–P	4^f	3.60	0.0064	2.4^g	
	U–O–P	8^f	3.70^g	0.007	2.4^g	
	U1	4^f	5.25	0.011	2.4^g	
	U2	4^f	6.88	0.011^g	2.4^g	
A: U : P = 1 : 3, pH = 2.6	U═O	2^f	1.78	0.0018	1.2	0.16
	U–O_{eq}	3.7	2.28	0.0019	1.2^g	
	U–P	3.7^g	3.58	0.0025	1.2^g	
	U–O_{eq} –P	7.4^g	3.68^g	0.0021	1.2^g	
	U1	3.7^g	5.22	0.0055	1.2^g	
	U2	3.7^g	6.86	0.0055	1.2^g	
B: U : P = 1 : 3, pH = 4.6	U═O	2^f	1.79	0.0017	1.0	0.23
	U–O_{eq}	3.1	2.29	0.0018	1.0^g	
	U–P	2.5	3.58	0.0025^f	1.0^g	
	U–O_{eq} –P	5.0^g	3.68^g	0.0021^f	1.0^g	
	U1	2.5^g	5.20	0.0055^f	1.0^g	
	U2	2.5^g	6.86	0.0055^f	1.0^g	
C: U : P = 1 : 3, pH = 7.0	U═O	2^f	1.79	0.0017	0.3	0.23
	U–O_{eq}	3.5	2.30	0.0032	0.3^g	
	U–P	2.2	3.58	0.0025^f	0.3^g	
	U–O_{eq} –P	4.4^g	3.68^g	0.0021^f	0.3^g	
	U1	2.2^g	5.20	0.009	0.3^g	
	U2	2.2^g	6.89	0.0055^f	0.3^g	
D: U : P = 5 : 3, pH = 3.9	U═O	2^f	1.79	0.0034	1.8	0.27
	U–O_{eq1}	2.7	2.33	0.0043	1.8^g	
	U–O_{eq2}	0.9	2.52	0.0043^g	1.8^g	

^{a} Coordination number. N ± ~20%. ^{b} Atomic distances. R ± ~0.02 Å. ^{c} Debye–Waller factor. ^{d} Energy shift parameter linked for all paths. ^{e} F-value as estimated by EXAFSPAK. ^{f} Fixed parameter. ^{g} Parameter linked proportionally to the parameter in the row above.

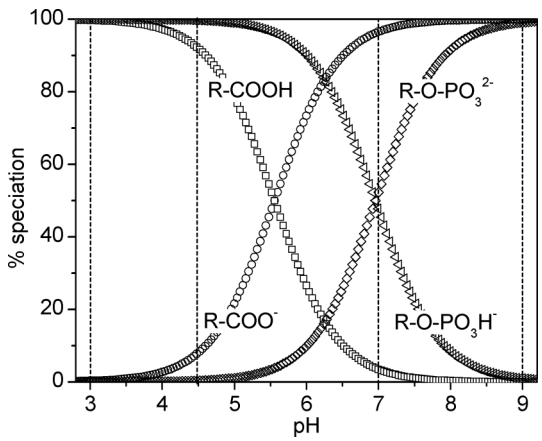

Fig. 3 Speciation of the protonated and deprotonated functional groups of LPS in dependency of pH, based on the pK_a values determined potentiometrically[6] (idealized illustration considering the deprotonation of different functional groups independently). Vertical dashed lines: pH values where IR spectra were measured.

to the U–P distances of 3.58 Å to 3.60 Å. These U–O_{eq} and U–P distances are characteristic values for four-fold monodentate coordination of phosphate groups[9,29] and were also found for uranium-treated bacteria.[8–10,12,13] From these investigations it was suggested that inorganic phosphate is released from the cells because of microbial activity resulting in a formation of an inorganic uranyl phosphate precipitates. In addition, strong FT peaks at around 5 Å and 6.6 Å are presumably due to U–U interactions at 5.2 Å and 6.9 Å. Furthermore, at around 4 Å a "doublet" peak structure can be observed which belongs to overlapping single and multiple scattering paths. A detailed description is provided in the ESI† (text, Fig. S1 and S2 and Table S1). These structural features are typical for a uranium coordination observed for inorganic uranyl phosphates like *meta*-autunite. However, our samples contained stable microbial material isolated from bacteria where the release of inorganic phosphate can be neglected. Moreover, an alternative U–P interaction type with longer U–O_{eq} distances and a five-fold coordination sphere has already been reported several times.[10,12–14,16,17,30] This U(VI) coordination was assigned to uranyl complexes with organic phosphate groups.

Because of these ambivalent results luminescence spectra were determined with the U(VI)-LPS samples used for EXAFS and uranyl phosphate and uranyl perchlorate serving as references (for experimental details and luminescence spectra, see ESI, text and Fig. S3†). From the spectra, uranyl complexes formed with either organic or inorganic phosphate ligands can be differentiated. The peak maxima of the U(VI)-LPS samples are red-shifted compared to those of the uranyl perchlorate sample; but the peaks in the spectrum of the inorganic uranyl phosphate complex are considerably more shifted to longer wavelengths. Moreover, the luminescence maxima of the U(VI)-LPS EXAFS samples fit very well with those of the U-LPS complexes in solution[6] and with other organic uranyl phosphates.[31–34] Therefore, we conclude that the EXAFS spectra of the U(VI)-LPS samples mainly represent uranyl complexes with organic phosphate groups. In these complexes, the interatomic distances in the first shell of the uranyl ion are obviously quite similar to those found for *meta*-autunite.

With respect to the high density of phosphoryl groups in the inner core region and lipid A of LPS (see Fig. 1), the formation of

both intra- and intermolecular uranyl phosphoryl coordination is plausible. A proposed coordination sphere of the uranyl ion is schematically depicted in Fig. 4. Such a combined intra- and intermolecular four-fold phosphoryl coordination of the uranyl ion in the three-dimensional LPS network can explain the U–U distances observed by EXAFS spectroscopy. Intermolecular ionic bridges between phosphoryl groups have already been observed with divalent cations like Ca^{2+} and Mg^{2+} which stabilizes the three-dimensional structure of LPS in bacterial cell walls.[35,36]

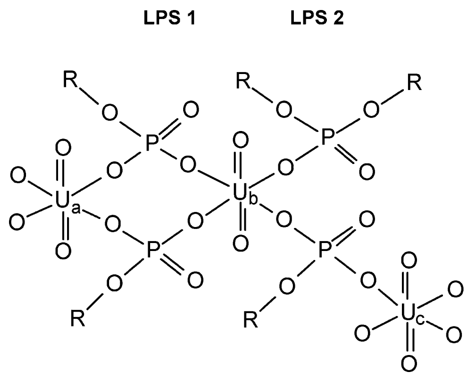

Fig. 4 Schematic illustration of the proposed structure of LPS bound uranyl from EXAFS results, demonstrating intra- and intermolecular four-fold monodentate phosphoryl coordination of the uranyl ion and explaining the different U–U distances listed in Table 2 (U1: U_a-U_b and U2: U_b-U_c).

Sample D, with a nearly equimolar ratio of uranyl and functional groups (sum of carboxyl and phosphoryl), corresponding to a deficit of phosphoryl groups, shows a completely different EXAFS spectrum compared to samples A–C. The best fit was obtained with two equatorial oxygen atoms at about 2.33 Å and 2.52 Å. Assuming phosphoryl and carboxyl groups represent the only binding sites for U(VI) as it was already demonstrated,[6] one can interpret the two different U–O distances as follows: The smaller distance is assigned to a monodentate phosphate binding in a five-fold equatorial coordination sphere,[14,16,29,31,37,38] whereas the larger value represents a bidentate coordination to carboxylate groups.[27,39,40] A bidentate phosphoryl coordination is also conceivable for such a high U–O distance value.[41] However, such coordination has not yet been observed in aquatic biological systems. Therefore, a coordination of additional water molecules to monodentate phosphoryl coordination seems more likely. Such a complex was already observed previously.[16,42]

In fact, the EXAFS spectrum of sample D provides no direct evidence of U–P interactions. Because of the strong destructive interference of the U–P path with the three-fold U–O–P multiple scattering path,[43] the intensity of the signal of one or two phosphate groups coordinated to the uranyl ion is expected to be of same magnitude as the experimental error, and the U–P interaction would be hardly observable. Moreover, we cannot provide clear evidence for the presence of a U–C interaction as a bidentate carboxylate coordination which is expected to show up about 2.9 Å in the FT of the EXAFS spectrum.[44–46] Because the noise level of the spectrum of sample D, particularly at higher k values, is much higher in comparison to the spectra of samples A–C, the U–C distance could not be resolved from the spectrum. This might be due to the presence of a mixed coordination mode in sample D, whereas a more predominant mode of U(VI) coordination can be found in sample A–C.

With EXAFS, the main structural features in the near field of the uranyl ion could be clearly identified for environmental conditions with LPS excess, equivalent to an excess of phosphoryl groups. We found a *meta*-autunite like four-fold coordination sphere with monodentate phosphoryl groups in the equatorial plane of the uranyl ion. The elucidation of the structure of the U(VI)-LPS complex with deficit of phosphoryl groups can not be provided by this technique. Therefore, vibrational spectroscopic investigations were carried out for the study of U(VI)-LPS complexes under such conditions.

ATR-FT-IR spectra of aqueous LPS at different pH values

Infrared spectra of complex biomolecules generally show overlapping bands which hamper an accurate interpretation of the observed spectral features. In order to differentiate between vibrational modes of the phosphoryl and carboxyl groups and modes of the carbohydrate ring systems of the LPS molecule, a series of spectra at selected pH values ranging from 3 to 9 was recorded. With respect to the chemical structure of LPS (Fig. 1), it can be expected that mainly carboxyl and phosphoryl groups are deprotonated within this spectral range, and, therefore, provoke distinct spectral changes which can be assigned to these groups.

The speciation of these functional groups was calculated from the previously determined pK_a values[6] and is depicted in Fig. 3 in an idealized form presuming that the different functional groups are deprotonated independently. From this result, it can be derived that most of the carboxyl groups are protonated and nearly all phosphoryl groups exist in their singly deprotonated form, $ROPO_3H^-$, below pH 3.5. At pH 5.5 and 7.0, about half of the carboxyl and phosphoryl groups are calculated to be deprotonated, respectively. Above pH 8, almost all phosphoryl groups are deprotonated.

The respective FT-IR spectra of the aqueous solutions of LPS are depicted in Fig. 5; the main absorption bands are summarized in Table 3. All IR spectra are characterized by strong bands around 1650 and 1550 cm^{-1} which can be attributed to the amide I and II modes of the LPS molecule. In the spectral region below 1250 cm^{-1}, additional strong and overlapping bands are observed which undergo significant changes upon increasing pH values. In this spectral region, characteristic bands of carbohydrates and phosphoryl groups are normally observed. Because of the broad and overlapping bands it is difficult to give an unequivocal assignment of these bands to distinct vibrational modes. In particular, in the pH range between 4.5 and 7, the shapes of the spectra are significantly changing in this spectral region (Fig. 5b, 5c). From the calculated speciation, it becomes obvious that these spectral alterations reflect the deprotonation of the phosphoryl groups. However, the deprotonation of the carboxyl groups was also determined to occur within this pH range (Fig. 3).

Because the spectral changes of these groups are hardly observed in the absorption spectra due to strongly interfering bands, we calculated a difference spectrum from the spectra recorded at pH 9 and 3. In this spectrum, positive and negative bands represent vibrational modes of the LPS molecule at high and low pH values, respectively (Fig. 5e). The change of the protonation state of the carboxyl groups can be clearly derived from this spectrum.

Table 3 Overview and tentative assignment of the infrared bands observed in the infrared spectra. Positive and negative bands of difference spectra are marked as (+) and (–), respectively. Indicated values are given in cm^{-1} [a]

Absorption spectra of LPS(aq.)				
pH 3.0 Fig. 5a	pH 4.5 Fig. 5b	pH 7.0 Fig. 5c	pH 9.0 Fig. 5d	Tentative assignment
1653	1655	1647	1641	Amide-I
1549	1541	1557	1554	Amide-II, $\nu_{as}(COO^-)$
—	1410	1406	1407	$\nu_s(COO^-)$
1230	1235	1247	1241	ν(P═O), δ(C–OH)
1112	1113 (sh)	1111	—	ν_{as}(P–O); $ROPO_3H^-$
—	—	1081	1083	ν_{as}(P–O); $ROPO_3^{2-}$
1065	1080	1055	—	ν_s(P–O); $ROPO_3H^-$
—	—	984 (sh)	—	ν_s(P–O); $ROPO_3^{2-}$

Difference spectra of aqueous solutions				
LPS	[U–LPS](+) – LPS(–)			
pH 9(+) – pH 3(–) Fig. 5e	pH 2.7 Fig. 6a	pH 4.5 Fig. 6b	pH 7.0 Fig. 6c	Tentative assignment
1700(–)	1715(–)	—	—	ν(COOH)
1576(+)	1537(+)	1528(+)/1559(–)	1535(+)/1558(–)	$\nu_{as}(COO^-)$
1404(+)	1455(+)	1458(+)/1404(–)	1453(+)/1404(–)	$\nu_s(COO^-)$
1221(–)	1236(–)	—	—	ν(P═O), δ(C–OH)
—	1200(+)	1209(+)	1216(+)	ν(P═O)
1067(–)	1114/1064(+)	1105/1057(+)	1147/1060/997(+)	ν(P–O)
987(+)	—	—	—	ν_s(P–O); $ROPO_3^{2-}$
962(–)	—	—	—	ν_{as}(P–OH); $ROPO_3H^-$
—	925(+)	923(+)	918(+)	$\nu_{as}(UO_2)$

[a] ν: stretching vibration; as: antisymmetric; s: symmetric; δ: bending vibration; sh: shoulder.

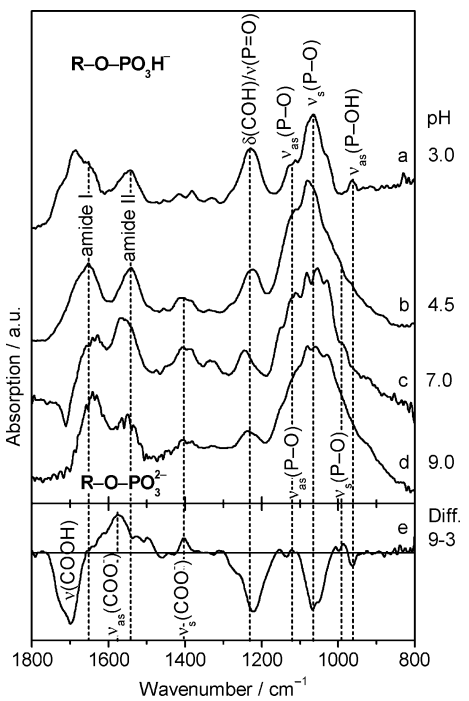

Fig. 5 Mid-IR spectra of aqueous solutions of LPS at different pH values. Spectra were recorded at pH 3.0 (a), 4.5 (b), 7.0 (c), and 9.0 (d). Difference spectrum calculated from the absorption spectra recorded at pH 9.0 and 3.0 (e).

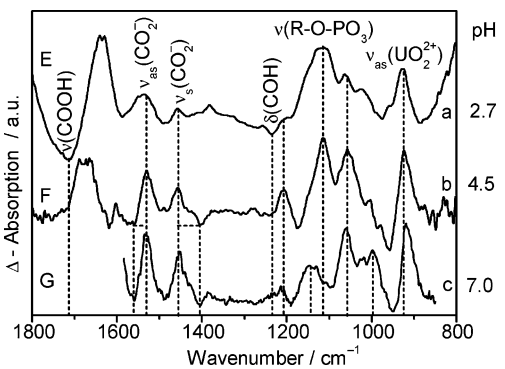

Fig. 6 Mid-IR difference spectra of aqueous uranyl LPS complexes. Sample E: U : P = 3 : 1, pH 2.7 (a); F: U : P = 2 : 1, pH 4.5 (b); G: U : P = 2 : 1, pH 7.0 (c). Positive and negative bands represent modes of the U–LPS and LPS molecules in aqueous solution, respectively. For compositions of samples see Table 1.

The negative band around 1700 cm^{-1} and the positive bands at 1576 and 1404 cm^{-1} are assigned to COOH at low pH and to the antisymmetric (ν_{as}) and symmetric (ν_s) stretching vibration of the carboxylate groups at higher pH, respectively. It has to be noted that the band at 1700 cm^{-1} is probably superimposed by spectral alterations of the water solvent which cannot be accurately subtracted.

In the region below 1250 cm^{-1}, the observed bands can be mainly attributed to modes of phosphoryl groups which are deprotonated upon increasing the pH from 3 to 9.[47,48] It was shown that

infrared spectra of carbohydrates generally show strong bands in this spectral range but their shapes do not significantly change within a wide pH range.[49] Nevertheless, the bands observed in this spectral range have to be considered as results of overlapping modes allowing only a preliminary assignment.

The band around 1230 cm^{-1} is assigned to the ν_{as}(P═O) mode. It generally shows decreasing relative intensity upon deprotonation of the phosphoryl group (Fig. 5a–d).[49] Additionally, the δ(C–OH) mode, which is expected to disappear upon deprotonation of the carboxyl groups, is generally observed as a broad band centred around 1250 cm^{-1}. Therefore, we consider the band around 1230 cm^{-1} as a superposition of these two modes. Consequently, this band is observed as a strong negative band in the respective difference spectrum (Fig. 5e).

With increasing pH, the strong band around 1055 cm^{-1} is broadened, representing not only modes of the protonated and deprotonated phosphoryl groups[48–51] but also increasing contributions from modes of the sugar rings (Fig. 5a–d). Even at pH 9, where all phosphoryl groups should be deprotonated, strong overlapping bands are still observed in this spectral region (Fig. 5d) which allows no accurate band assignments.

However, from the calculated difference spectrum, information about distinct functional groups can be derived. The spectrum shows strong negative bands at 1067 and 965 cm^{-1} and a small positive band at 965 cm^{-1}. The former bands can be mainly attributed to the P–O stretching and antisymmetric P–OH vibration mode of the hydrogenphosphate group, respectively, whereas the latter band represents the symmetric P–O vibration of the deprotonated phosphoryl group.[50] The lack of a positive band around 1115 cm^{-1}, which is expected to represent the ν_{as}(P–O) mode of the deprotonated phosphoryl group,[48,49] is most likely due to an unsatisfactory spectrum subtraction due to the presence of strong overlapping modes of the numerous sugar ring moieties in this spectral region.

The spectra of LPS recorded at different pH values obviously confirm qualitatively the calculated result of the speciation shown in Fig. 3. The most significant spectral changes are observed between the spectra recorded at pH 4.5 and 7 where most of the functional groups are predicted to change their protonation states. From the spectra, the frequencies of the modes of the uncomplexed carboxylate groups can be derived and the spectral features in the spectral range of the organic phosphate groups might be helpful for the interpretation of the spectra of the LPS-U(VI) complexes presented in the following section.

ATR-FT-IR spectra of uranyl LPS complexes

While the high affinity of the uranyl ion to phosphoryl groups is well-known, studies on the influence of the carboxyl groups beside phosphoryl groups on the complex behaviour of bio systems are very scarce.[15–17,48] Therefore, samples containing nearly equimolar ratio of uranyl and functional groups (sum of carboxyl and phosphoryl, see Table 1) of LPS were investigated at three different pH values between 2.7 and 7.0. Under these conditions, a coordination of the uranyl ion to carboxyl groups can be expected.

The difference spectra of uranyl LPS complex solutions *versus* free LPS are depicted in Fig. 6. These spectra only show bands of vibrational modes which undergo changes upon metal complexation. Positive and negative bands represent the samples of the uranyl LPS complex and of the uncomplexed LPS, respectively. The main bands observed are summarized in Table 3.

Vibrational modes of the carboxylate groups. The affinity of the uranyl ion to carboxylate groups is reflected in the difference spectra of the U–LPS complexes. All spectra between pH 2.7 and 7.0 show positive bands at about 1535 and 1455 cm^{-1} which can be assigned to the ν_{as} and ν_{s} stretching modes of the carboxylate groups, respectively. Consequently, the negative bands at 1715 and 1236 cm^{-1} observed in the spectrum recorded at pH 2.7 (sample E, Fig. 6a) can be attributed to the ν(COOH) and δ(C–OH) mode of the carboxyl groups of the LPS molecule, respectively. These groups are deprotonated upon U(VI) complexation and, hence, the corresponding positive bands of the ν_{as} and ν_{s} modes of the COO^{-} groups are observed.

In the spectra recorded at higher pH values, that is at pH 4.5 and 7.0 (Fig. 6b, 6c), these modes are observed as negative bands around 1560 and 1404 cm^{-1} representing the uncomplexed LPS and as positive bands around 1530 and 1455 cm^{-1} reflecting characteristic frequency shifts of these modes upon U(VI) complexation.[22,52] The decrease of the spectral splitting of the ν_{as} and ν_{s} modes in the uranyl complexes ($\Delta\nu \approx 75$ cm^{-1}) compared to the uncomplexed LPS ($\Delta\nu \approx 155$ cm^{-1}) is characteristic of the formation of a bidentate coordination of the uranyl ion in carboxyl complexes.[22,52]

In a recent study of the main saccharic acid building blocks of LPS, the frequencies of vibrational modes of carboxyl groups, uncomplexed and complexed with various metal ions, were determined by quantum chemical calculations.[53] For a bidentate coordination of U(VI) with Kdo (2-keto-3-deoxyoctanoate), a spectral splitting of $\Delta\nu = 116$ cm^{-1} was calculated whereas for galacturonate only $\Delta\nu = 54$ cm^{-1} was obtained. The experimental data of our work ($\Delta\nu \approx 75$–80 cm^{-1}), therefore, might be interpreted as the formation of bidendate U(VI) complexes with carboxyl groups originating from different saccharic binding sites of the LPS molecule.

Vibrational modes of the organic phosphate groups. The spectral region, where the asymmetric and symmetric stretching of P–O modes of the phosphoryl groups are expected, shows an intense broad positive band at 1114 cm^{-1} and a smaller one at 1054 cm^{-1} in the spectrum recorded at pH 2.7 (Fig. 6a). Both bands are of same intensity at pH 4.5 (Fig. 6b). At pH 7.0, the latter one increases, whereas the former one disappears completely and two new modes show up at 1147 and 995 cm^{-1} (Fig. 6c), which are already observed as a small band and as a shoulder at pH 4.5, respectively (Fig. 6b).

Distinct structural changes of the functional groups upon uranium(VI) coordination can not be derived in detail because conformational changes of the carbohydrate framework have to be considered and might contribute significantly to the spectra. It can be expected that numerous phosphoryl groups with different molecular environments contribute to the vibrational bands and, therefore, hampers an unequivocal assignment. Nevertheless, from the spectra of pure LPS recorded at different pH values, spectral changes between 1220 and 960 cm^{-1} were assigned to phosphoryl groups (Fig. 5). Consequently, a coordination of uranyl ions to phosphoryl can be derived from the difference spectra of the U–LPS complexes because of the observed significant absorption changes in this frequency range. The pH dependent change of the band pattern might reflect the formation of different

U(VI)-phosphoryl complexes with respect to the prevailing speciation of the phosphoryl groups.

From our recent study of U(VI) complexation with the highly phosphorylated, naturally occurring protein phosvitin,[48] a similar band pattern was observed for a corresponding sample of a similar U/P ratio at pH 4 at slightly lower frequencies. These spectral homologies strongly suggest the coordination of the uranyl ion to phosphoryl groups. The observed alterations in band positions might be due to the different character of the phosphoryl groups, that is saccharic residues in LPS *vs.* amino acidic side chain residues in phosvitin.

Vibrational mode of the UO_2^{2+} group. The antisymmetric stretching vibration of the UO_2^{2+} cation can be observed as strong bands around 920 cm^{-1} in all spectra of the U–LPS complexes (Fig. 6a–c). A small absorption band at 960 cm^{-1} in the spectrum at pH 2.7 is assigned to the fully hydrated uranyl ion[52,54,55] indicating the presence of uncomplexed uranyl under the prevailing conditions.

Complexation of uranyl provokes a strong bathochromic shift of the $\nu_{as}(UO_2)$ mode. A frequency of 925 cm^{-1} (pH 2.7) is characteristic for complexation of uranyl with carboxylate groups.[22,52,55] Furthermore, the presence of uranyl hydroxide species effects also a shift of this mode to about 925 cm^{-1} at pH values > 3 in the lower millimolar concentration range.[54] However, at pH values below 3, the dominant absorption band of aqueous uranyl solutions is found at 961 cm^{-1}.[54,55] Hence, the presence of the band around 925 cm^{-1} in the spectrum of the U–LPS complex recorded at pH 2.7 can only be explained by a complexation of uranyl to the functional groups of LPS at this pH level. Because of the significant absorption changes of carboxyl and phosphoryl bands in the spectra of the U–LPS complexes, an extensive coordination of uranyl to both functional groups is suggested. Consequently, the band at 925 cm^{-1} represents both a complexation to carboxyl and phosphoryl groups.

With increasing pH, the band of the uranyl mode is further shifted to 923 cm^{-1} showing a small shoulder at 915 cm^{-1} at pH 4.5 (Fig. 6b). At pH 7.0, the maximum of this band is observed at 918 cm^{-1} (Fig. 6c). It is assumed that the bathochromic shift is caused by increasing contributions of phosphoryl coordination related to carboxyl coordination. A similar shift of the $\nu_{as}(UO_2^{2+})$ mode was very recently observed for the uranyl phosvitin complex system.[48]

Summary and conclusion

We have obtained a detailed and widespread overview of the uranyl binding properties with LPS in the mildly acidic to neutral pH range. At very low uranyl concentrations, corresponding to an excess of LPS and its functional groups, we observe coordination with mainly phosphoryl groups as it was derived from EXAFS results. At a higher relative amount of uranyl, corresponding to a reduced ratio of LPS functional groups, an additional significant coordination to carboxylate groups can be observed as it was proven by IR spectroscopy. Up to now, investigations, focusing on bacterial cells and cell walls of both Gram-positive and Gram-negative bacteria, have shown a simultaneous coordination of U(VI) to phosphoryl and carboxyl groups, but only at fixed pH values of 4.5 and 5.0, respectively.[15,17]

In this study, we were able to elucidate the affinity of uranyl to these two different coordinating functional groups: phosphoryl groups preferentially coordinate the uranyl ion already at very low metal concentrations, obviously in a monodentate manner. Contributions from carboxylate groups to the coordination of uranyl become relevant at equimolar conditions related to the functional groups of LPS. The carboxylate group is suggested to bind bidentately to uranyl ion. The affinity of U(VI) to phosphoryl groups seems to increase slightly with increasing pH.

These findings are contradictory to results obtained from Gram-positive bacteria cell walls[16] where a decrease of phosphoryl and an increase of carboxyl coordination with increasing pH (from 1.7 up to 4.8) was derived. In fact, Gram-positive bacteria do not contain LPS and, thus, provide only a relative low amount of phosphoryl groups. Therefore, the U(VI) binding sites of Gram-negative bacteria cell walls is predominantly controlled by LPS.

From a recently published computer simulation study of uranyl uptake by LPS[21] it was assumed that at neutral pH the uranyl ion would be retained in the outer core through chelating with carboxyl and hydroxyl groups. As it is stated by the authors, the contradictory results might be due to the fact that earlier investigations were exclusively carried out at lower pH. In this study, we could clearly show the predominant contribution of phosphoryl groups to uranyl complexation even at neutral pH. However, the calculations were carried out for the complexation of the aquatic uranyl cation $UO_2(H_2O)_5^{2+}$ with LPS strains embedded in a fixed cell-wall-like matrix,[21] whereas in this study isolated LPS strains are considered. Possibly, the flexibility of fixed LPS strains is limited and impedes the migration of metal ions to the inner core where the majority of the phosphoryl groups are located. On the other hand, the speciation of the uranyl ion particularly at neutral pH is very complex and not fully understood today. Several hydroxo and carbonate species have to be considered during the modelling of U(VI) complexation which might have a significant impact on the calculated results of U(VI) complexation with the functional groups of LPS.

Our study constitutes an important contribution towards the better understanding of metal binding behaviour with microbial material. From the results, it can be presumed that isolated LPS might have a higher binding capacity towards uranium than when embedded in an intact cell wall. Hence, dead cells which release a high amount of various biopolymers, might have a greater influence of the migration behaviour of uranium than living bacteria. Additionally, we also provide a precise basis for future computer simulations. Continuative investigations with bacterial cell wall compartments are necessary for an enhancement of the effectiveness of microbial systems for bioremediation technologies.

Acknowledgements

This work was partly funded by the German Federal Ministry of Economics and Technology (BMWi) under contract number 02E9985.

References

1 L. E. Macaskie, J. R. Lloyd, R. A. P. Thomas and M. R. Tolley, *Nucl. Energy-J. Br. Nucl. Energy Soc.*, 1996, **35**, 257–271.
2 T. Barkay and J. Schaefer, *Curr. Opin. Microbiol.*, 2001, **4**, 318–323.

3 J. C. Renshaw, J. R. Lloyd and F. R. Livens, *C. R. Chim.*, 2007, **10**, 1067–1077.
4 M. L. Merroun and S. Selenska-Pobell, *J. Contam. Hydrol.*, 2008, **102**, 285–295.
5 Y. A. Knirel, O. V. Bystrova, N. A. Kocharova, U. Zahringer and G. B. Pier, *J. Endotoxin Res.*, 2006, **12**, 324–336.
6 A. Barkleit, H. Moll and G. Bernhard, *Dalton Trans.*, 2008, 2879–2886.
7 Y. Andres, H. J. MacCordick and J.-C. Hubert, *FEMS Microbiol. Lett.*, 1994, **115**, 27–32.
8 M. J. Beazley, R. J. Martinez, P. A. Sobecky, S. M. Webb and M. Taillefert, *Environ. Sci. Technol.*, 2007, **41**, 5701–5707.
9 C. Hennig, S. Selenska-Pobell, W. Matz and P. Panak, *Radiochim. Acta*, 2001, **89**, 625–631.
10 F. Jroundi, M. L. Merroun, J. M. Arias, A. Rossberg, S. Selenska-Pobell and M. T. Gonzalez-Munoz, *Geomicrobiol. J.*, 2007, **24**, 441–449.
11 L. E. Macaskie, K. M. Bonthrone, P. Yong and D. T. Goddard, *Microbiology-(UK)*, 2000, **146**, 1855–1867.
12 M. Merroun, M. Nedelkova, A. Rossberg, C. Hennig and S. Selenska-Pobell, *Radiochim. Acta*, 2006, **94**, 723–729.
13 M. Nedelkova, M. L. Merroun, A. Rossberg, C. Hennig and S. Selenska-Pobell, *FEMS Microbiol. Ecol.*, 2007, **59**, 694–705.
14 M. Merroun, C. Hennig, A. Rossberg, T. Reich and S. Selenska-Pobell, *Radiochim. Acta*, 2003, **91**, 583–591.
15 A. J. Francis, J. B. Gillow, C. J. Dodge, R. Harris, T. J. Beveridge and H. W. Papenguth, *Radiochim. Acta*, 2004, **92**, 481–488.
16 S. D. Kelly, K. M. Kemner, J. B. Fein, D. A. Fowle, M. I. Boyanov, B. A. Bunker and N. Yee, *Geochim. Cosmochim. Acta*, 2002, **66**, 3855–3871.
17 M. L. Merroun, J. Raff, A. Rossberg, C. Hennig, T. Reich and S. Selenska-Pobell, *Appl. Environ. Microbiol.*, 2005, **71**, 5532–5543.
18 M. Carriere, O. Proux, S. Milgram, C. Thiebault, L. Avoscan, N. Barre, C. Den Auwer and B. Gouget, *J. Biol. Inorg. Chem.*, 2008, **13**, 655–662.
19 L. Avoscan, S. Milgram, G. Untereiner, R. Collins, H. Khodja, J. Coves, J. L. Hazemann, M. Carriere and B. Gouget, *Radiochim. Acta*, 2009, **97**, 375–383.
20 C. C. Fuller, J. R. Bargar and J. A. Davis, *Environ. Sci. Technol.*, 2003, **37**, 4642–4649.
21 R. D. Lins, E. R. Vorpagel, M. Guglielmi and T. P. Straatsma, *Biomacromolecules*, 2008, **9**, 29–35.
22 A. Barkleit, H. Foerstendorf, K. Heim, S. Sachs and G. Bernhard, *Appl. Spectrosc.*, 2008, **62**, 798–802.
23 T. Reich, G. Bernhard, G. Geipel, H. Funke, C. Hennig, A. Rossberg, W. Matz, N. Schell and H. Nitsche, *Radiochim. Acta*, 2000, **88**, 633–637.
24 G. N. George and I. J. Pickering, *EXAFSPAK: a suite of computer programs for analysis of X-ray absorption spectra*, Stanford Synchrotron Radiation Laboratory, Stanford, CA, 2000.
25 A. L. Ankudinov, B. Ravel, J. J. Rehr and S. D. Conradson, *Phys. Rev. B: Condens. Matter Mater. Phys.*, 1998, **58**, 7565–7576.
26 E. S. Makarov and V. I. Ivanov, *Doklady Akademii Nauk Sssr*, 1960, **132**, 673–676.
27 D. H. Templeton, A. Zalkin, H. Ruben and L. K. Templeton, *Acta Crystallogr., Sect. C: Cryst. Struct. Commun.*, 1985, **41**, 1439–1441.
28 Z. Szabo, T. Toraishi, V. Vallet and I. Grenthe, *Coord. Chem. Rev.*, 2006, **250**, 784–815.
29 P. C. Burns, *Can. Mineral.*, 2005, **43**, 1839–1894.
30 M. L. Merroun, G. Geipel, R. Nicolai, K. H. Heise and S. Selenska-Pobell, *BioMetals*, 2003, **16**, 331–339.
31 A. Koban, G. Geipel, A. Rossberg and G. Bernhard, *Radiochim. Acta*, 2004, **92**, 903–908.
32 A. Koban and G. Bernhard, *Polyhedron*, 2004, **23**, 1793–1797.
33 A. Koban and G. Bernhard, *J. Inorg. Biochem.*, 2007, **101**, 750–757.
34 A. Günther, G. Geipel and G. Bernhard, *Radiochim. Acta*, 2006, **94**, 845–851.
35 M. Schindler and M. J. Osborn, *Biochemistry*, 1979, **18**, 4425–4430.
36 P. L. Kotra, D. Golemi, N. A. Amro, G. Liu and S. Mobashery, *J. Am. Chem. Soc.*, 1999, **121**, 8707–8711.
37 J. H. Burns, *Inorg. Chem.*, 1983, **22**, 1174–1178.
38 G. J. Vazquez, C. J. Dodge and A. J. Francis, *Chemosphere*, 2007, **70**, 263–269.
39 A. Rossberg, L. Baraniak, T. Reich, C. Hennig, G. Bernhard and H. Nitsche, *Radiochim. Acta*, 2000, **88**, 593–597.
40 A. Rossberg, T. Reich and G. Bernhard, *Anal. Bioanal. Chem.*, 2003, **376**, 631–638.
41 R. J. Francis, M. J. Drewitt, P. S. Halasyamani, C. Ranganathachar, D. O'Hare, W. Clegg and S. J. Teat, *Chem. Commun.*, 1998, 279–280.
42 G. J. Vazquez, C. J. Dodge and A. J. Francis, *Inorg. Chem.*, 2008, **47**, 10739–10743.
43 C. Den Auwer, M. C. Charbonnel, M. T. Presson, C. Madic and R. Guillaumont, *Polyhedron*, 1998, **17**, 4507–4517.
44 M. A. Denecke, T. Reich, M. Bubner, S. Pompe, K. H. Heise, H. Nitsche, P. G. Allen, J. J. Bucher, N. M. Edelstein and D. K. Shuh, *J. Alloys Compd.*, 1998, **271**, 123–127.
45 T. I. Docrat, J. F. W. Mosselmans, J. M. Charnock, M. W. Whiteley, D. Collison, F. R. Livens, C. Jones and M. J. Edmiston, *Inorg. Chem.*, 1999, **38**, 1879–1882.
46 E. H. Bailey, J. F. W. Mosselmans and P. F. Schofield, *Geochim. Cosmochim. Acta*, 2004, **68**, 1711–1722.
47 S. J. Parikh and J. Chorover, *Colloids Surf., B*, 2007, **55**, 241–250.
48 B. Li, J. Raff, A. Barkleit, G. Bernhard and H. Foerstendorf, *J. Inorg. Biochem.*, 2010, **104**, 718–725.
49 W. Jiang, A. Saxena, B. Song, B. B. Ward, T. J. Beveridge and S. C. B. Myneni, *Langmuir*, 2004, **20**, 11433–11442.
50 M. C. Zenobi, C. V. Luengo, M. J. Avena and E. H. Rueda, *Spectrochim. Acta, Part A*, 2008, **70**, 270–276.
51 M. C. Zenobi, C. V. Luengo, M. J. Avena and E. H. Rueda, *Spectrochim. Acta, Part A*, 2010, **75**, 1283–1288.
52 M. Kakihana, T. Nagumo, M. Okamoto and H. Kakihana, *J. Phys. Chem.*, 1987, **91**, 6128–6136.
53 P. Selvarengan, J. D. Kubicki, J. P. Guegan and X. Chatellier, *Chem. Geol.*, 2010, **273**, 55–75.
54 K. Müller, V. Brendler and H. Foerstendorf, *Inorg. Chem.*, 2008, **47**, 10127–10134.
55 F. Quilès and A. Burneau, *Vib. Spectrosc.*, 1998, **18**, 61–75.

